3D-printed geometric distortion correction phantom for MRI

David W Holdsworth[1,2], Matthew G Teeter[1,2], Jaques S Milner[2], Steven I Pollmann[2], and Maria Drangova[2,3]
[1]Department of Surgery, Western University, London, Ontario, Canada, [2]Robarts Research Institute, London, Ontario, Canada, [3]Department of Medical Biophysics, Western University, London, Ontario, Canada

TARGET AUDIENCE: Researchers and clinicians in the field of MRI-guided intervention and surgical planning, including the development of patient-specific positioning guides, with a need to characterize and correct for inherent geometric distortions.

PURPOSE: The capability for routine and accurate characterization – and correction – of geometric distortion is becoming increasingly important for MRI applications in image-guided therapy. Applications where accurate geometrical measurements from MRI images are required include image-guided radiotherapy,[1] quantitative brain imaging,[2] and quantification during imaging for osteoarthritis[3] and the preparation of patient-specific positioning guides.[4] In order to correct for inherent geometric distortion, a variety of fiducial grids and sheets have been proposed, typically based on regularly structured 3D grids[5,6] or 3D distributions of glass marker beads.[7] Grid phantoms based on commercially fabricated polystyrene grids suffer from manufacturing imprecision and difficulty in post-processing and analysis to determine line intersections. Glass marker beads placed in custom-fabricated trays are complicated to fabricate. Recent advances in rapid prototyping – or "3D printing" – have made it possible to create accurate plastic structures of any desired 3D shape, facilitating an entirely new design of geometric distortion phantom. We have used 3D printing techniques to design and fabricate a 3D grid phantom, comprised of beads supported by cylindrical struts at known spacing. When immersed in a liquid, the phantom provides images that facilitate automated segmentation and analysis of the 3D distortion field within an image.

METHODS: The proposed distortion phantom is comprised of 4.5 mm diameter spheres, supported by 1.5 mm diameter cylindrical struts on nominal 13 mm spacing. A prototype version of this phantom, consisting of a 9 x 5 x 5 matrix, was fabricated using 3D printing (Objet 30 Pro, Stratasys) with a transparent resin (VeroClear, Stratasys). The 3D printer is designed to print over a 30 x 20 x 15 cm volume, with accuracy of ±0.1 mm. After fabrication, the 3D plastic construct (Fig. 1a) was immersed in a tissue-mimicking paramagnetic fluid to provide appropriate background signal, with $T1 < 200$ ms. A copper sulphate solution (7.8 mmol) in saline was used, following the description of Och *et al*.[8] Images were acquired at 3T (Discovery 750, GE Medical Systems) with a multi-channel knee coil, using a 3D turbo spin-echo sequence (CUBE, TR = 2300 ms, TE = 90 ms, flip angle = 90°, 0.7 mm slice thickness, 0.7 mm in-plane resolution, 128 kHz readout bandwidth, matrix size 320×320×160). To improve the accuracy of image segmentation, the resulting images were corrected for signal-intensity drop-off in the axial and trans-axial directions, using fitted parabolic functions. The resulting images of a dark grid on a bright background (Fig. 1b) were interpolated to isotropic 0.15 mm resolution and segmented based on a grey-scale threshold (Fig. 1c). To isolate individual fiducial locations within the grid, the segmented (binary) image was morphologically eroded to remove the struts, while retaining the beads at each intersection. In our case, erosion by an 8-pixel kernel removed 1.2 mm from every surface, thereby completely removing the struts and reducing the spheres to 2 mm diameter, as shown in Fig. 1d. Each of the 175 spheres was then identified and centroided to create a 3D point cloud of observed grid locations. These measured locations were subsequently compared to the best-fit locations of a synthesized grid, based on the known grid spacing. This produced a 3D vector map of sub-voxel geometric deviation throughout the image volume.

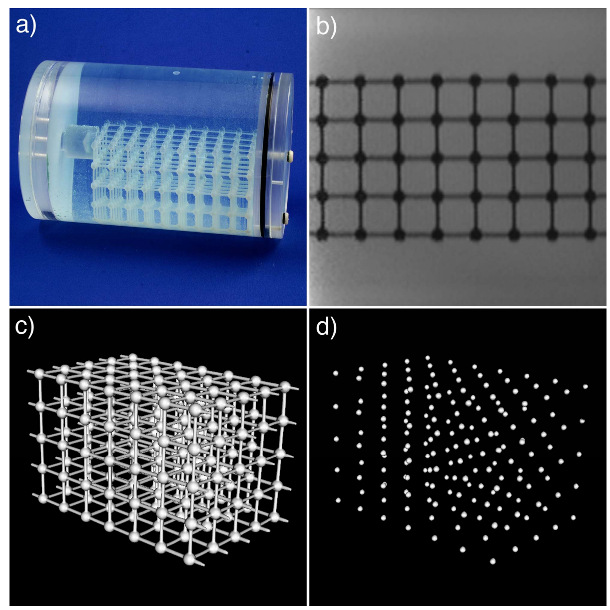

Fig. 1 (a) the prototype distortion grid phantom, sealed within the 12 cm diameter liquid enclosure; (b) MRI image through the central fiducial bead plane; (c) isosurface of a segmented grid image; (d) isosurface after morphological erosion by 1.2 mm.

RESULTS and DISCUSSION: The fabricated plastic grid phantom was evaluated for geometric accuracy using a measuring microscope (STM-6, Olympus) and a micro-CT scanner (eXplore Ultra, GE Healthcare). The measured fiducial spacing was determined to be 13.079 mm, within ±0.6% of the nominal value. Micro-CT analysis showed that fiducial centroids were within ±0.14 mm of their prescribed locations, on average. The grid phantom exhibited a low volumetric packing fraction within the background liquid, displacing less than 5% of the imaging volume. The small amount of material in the plastic grid ensures that the derived distortion vector map is relatively undisturbed by susceptibility artifacts. The derived geometric deviation map over the 11.7 x 6.5 x 6.5 cm^3 volume showed average geometric deviations of 0.53 mm, ranging from 0.11 to 1.20 mm.

CONCLUSION: 3D printing in MRI-compatible plastic resin has been used to fabricate and evaluate a geometric distortion phantom for MRI imaging. The grid structure provides a rigid and accurate phantom, which produces images that are amenable to fully automated quantitative analysis. This approach will be useful in any clinical application where geometric accuracy is important, either in routine quality assurance or as a component of distortion correction utilities.

REFERENCES: **1.** Crijns SP, et al. Towards inherently distortion-free MR images for image-guided radiotherapy on an MRI accelerator. *Phys Med Biol.* 2012; 57:1349-1358; **2.** Maikusa N, et al. Improved volumetric measurement of brain structure with a distortion correction procedure using an ADNI phantom. *Med Phys.* 2013; 40:062303; **3.** Schneider E, et al. The Osteoarthritis Initiative (OAI) magnetic resonance imaging quality assurance update. *Osteoarthritis Cartilage.* 2013; 21:110-116; **4.** Krishnan SP, et al. A review of rapid prototyped surgical guides for patient-specific total knee replacement. *J Bone Joint Surg Br.* 2012; 94:1457-1461; **5.** Baldwin LN, et al. Characterization, prediction, and correction of geometric distortion in 3 T MR images. *Med Phys.* 2007; 34:388-399; **6.** Wang D, et al. Geometric distortion in clinical MRI systems Part I: evaluation using a 3D phantom. *Magn Reson Imaging.* 2004; 22:1211-1221; **7.** Viard R, et al. Characterization and 3D correction of geometric distortion in open-magnet MRI. *Conf Proc IEEE Eng Med Biol Soc.* 2008; 2008:3649-3652; **8.** Och JG, et al. Acceptance testing of MRI systems: report of AAPM Nuclear Magnetic Resonance Task Group No. 6. *Med Phys.* 1992; 19:217-229.